VIP Heterogeneous Catalysis

DOI: 10.1002/anie.201007108

Morphology-Dependent Interactions of ZnO with Cu Nanoparticles at the Materials' Interface in Selective Hydrogenation of CO_2 to CH_3OH**

Fenglin Liao, Yaqun Huang, Junwei Ge, Weiran Zheng, Karaked Tedsree, Paul Collier, Xinlin Hong, and Shik C. Tsang**

In recent years, carbon dioxide (CO_2) has become the focus of much attention because of the position of CO_2 as the primary greenhouse gas and the implication of its emissions on the problem of climate change.[1] Various sequestration technologies for CO_2 abatement are being considered. It has been recently demonstrated that hydrogen gas can be manufactured on large scales from renewable sources, including solar energy, hydropower, and biomass.[2] Thus, complete or partial recycling of CO_2 through its hydrogenation to high-energy-density liquid fuels appears to be a very attractive approach. As a result, catalytic CO_2 hydrogenation reactions to methanol, higher alcohols, gasoline, and related higher hydrocarbons (Fischer–Tropsch-like reactions) have been receiving much renewed attention. Particularly, the focus is on the production of methanol, which is a key platform chemical for present fuel and chemical infrastructures.[3] A recent assessment of economic feasibility for this new green process supports the possibility.[4]

Today, methanol is produced industrially from syngas containing CO and CO_2 (derived from fossil fuels) over Cu/ZnO/Al_2O_3 catalysts.[5,6] These Cu/ZnO based systems are also evaluated to be the most efficient catalysts for the direct hydrogenation of CO_2 [Eq. (1)].[7] Although the two reactions

$$CO_2 + 3\,H_2 \rightleftharpoons CH_3OH + H_2O \qquad (1)$$

are likely to share a very similar mechanism (some works suggested CO_2 is the actual species for the production of methanol from syngas[6]), the relatively high concentration of CO_2 and H_2 in the carbon dioxide hydrogenation reaction also promotes the reverse water gas shift reaction to give CO [Eq. (2)], leading in general to a poorer methanol selectivity

$$CO_2 + H_2 \rightleftharpoons CO + H_2O \qquad (2)$$

than the syngas route. It would be useful to gain an understanding of the structure–activity relationships at the Cu–ZnO interface for these fundamentally important reactions.

Currently, morphology (shape) control in nanocatalysts has clearly suggested that catalysis is controlled not only by the chemical composition and size of the catalyst used but also by the type of surface sites available at the catalyst surface.[8] These considerations add exciting variables in tailoring the properties of nanocatalysts for a wide range of catalytic reactions. So far, only several examples of single-component metal nanocrystals and semiconductor oxide nanocrystals have been demonstrated,[8,9] but the role of shape control at the materials' interface, which is the common feature in practical metal-supported catalysts, is not yet known.

Herein, we present a significant shape effect of ZnO on its interaction with copper in the synthesis of methanol from carbon dioxide hydrogenation. The exposed polar (002) face in platelike ZnO shows a much stronger material synergy with copper than other crystal facets, which gives higher selectivity towards methanol from CO_2 hydrogenation. Electron paramagnetic resonance (EPR) clearly indicates a strong electronic interaction at the interface of the two materials, rendering it more selective for carbon dioxide activation and hydrogenation. It is envisaged that this new finding could lead to the rational design of new nanocatalysts for the potential use in carbon dioxide hydrogenation.

The syntheses of ZnO nanocrystals of platelike and rod shapes were based on published methods.[10,11] XRD analysis confirmed that they all show crystalline wurtzite structure (see the Supporting Information). The intensity of the (002) peak of truncated platelike ZnO nanoparticles was higher than other morphologies with the predominant polar facets covering the structure, whereas the extended rod structure showed relatively higher proportions of nonpolar (100) and (101) planes along the [0001] rod axis, as previously reported.[9]

The TEM image in Figure 1a reveals platelike ZnO with the diameter of 50–60 nm, and Figure 1b shows 600–800 nm rod-shaped ZnO with diameter of 20–30 nm. These images demonstrate that the uniform ZnO nanoparticles of rod and plate morphology were prepared by controlled nanochemical

[*] F. Liao, Y. Huang, J. Ge, W. Zheng, Dr. X. Hong, Prof. S. C. Tsang
College of Chemistry and Molecular Sciences
Wuhan University, Wuhan 430072 (China)
E-mail: edman.tsang@chem.ox.ac.uk
hongxl@whu.edu.cn
K. Tedsree, Prof. S. C. Tsang
Wolfson Catalysis Centre, Department of Chemistry
University of Oxford, Oxford, OX1 3QR (UK)
P. Collier
Johnson Matthey Technology Centre
Blount's Court Road, Sonning Common, Reading, RG4 7NH (UK)

[**] This research was financially supported by the NSFC-20903074 and the Fundamental Research Funds for the Central Universities. The authors thank Dr. J. Harmer of Oxford for EPR spectra; Y.H. thanks NSFC of China for a postdoctoral fellowship, and a studentship for K.T. from the Thai government is acknowledged.

Supporting information for this article is available on the WWW under http://dx.doi.org/10.1002/anie.201007108.

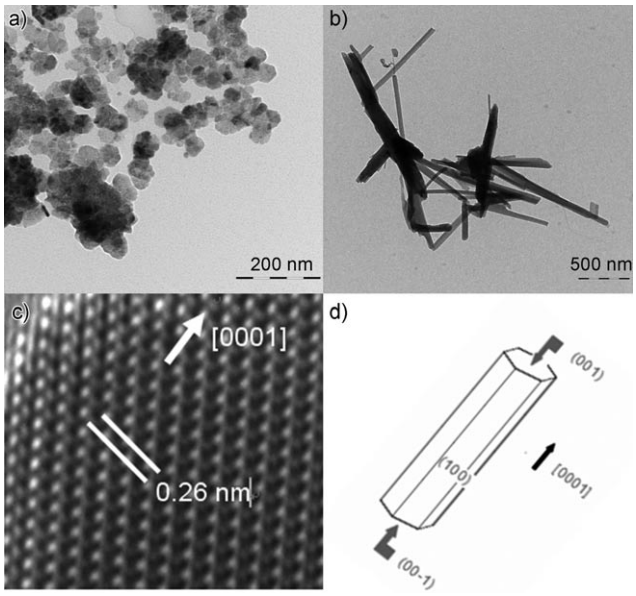

Figure 1. TEM images of a) ZnO plate particles; b) ZnO nanorods. c) HRTEM image of ZnO rod. d) Crystallographic relationship between ZnO plate and rod.

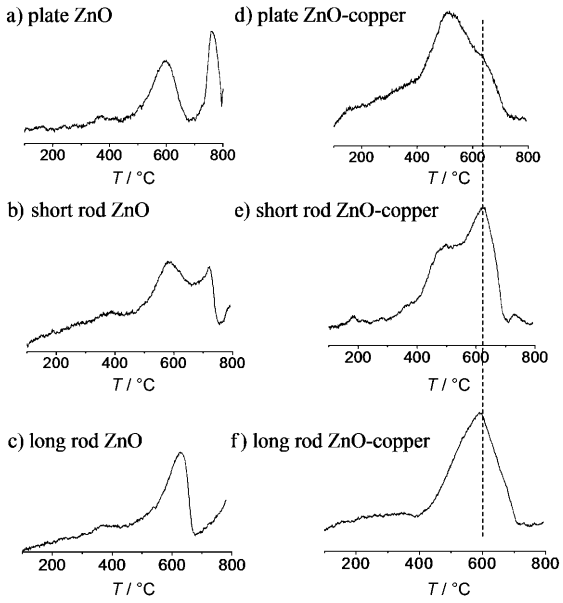

Figure 2. TPR curves of a) platelike; b) 400 nm rod ZnO; c) 600–800 nm rod ZnO, and their corresponding mixtures with copper (d–f).

synthesis.[9–11] It has been long believed that Cu displays a strong interaction with ZnO and that the materials' interface can generate active sites in traditional methanol synthesis, but there is a lack of direct experimental evidence. To characterize the interface, 35 nm Cu nanoparticles were synthesized and physically mixed with ZnO nanoparticles to avoid preferred deposition on any specific surface. It was anticipated that physical mixtures do not give as extensive and good interfaces as industrial catalysts but they serve as model materials for this study. The interactions between Cu and the two forms of ZnO, respectively, were probed by temperature-programmed reduction (TPR), as shown in Figure 2. There are two types of reducible oxygen atoms in the ZnO structure, which are reduced at 600 °C and 750 °C, respectively. Analyzing the relative proportions of these two peaks with references to their predominant exposed facets over these samples suggest that the 750 °C peak is associated with lattice oxygen atoms from the dominant (002) polar facet in ZnO plate, whereas the 600 °C peak arises from oxygen reduction from nonpolar facets (100, 110) in the rods. The 600 °C peak (nonpolar facets) changed marginally when mixed with Cu, suggesting that the nonpolar surfaces display poor interaction with the Cu phase. In a sharp contrast, the 750 °C peak almost disappeared when ZnO plate was mixed with Cu, and a new broad reduction peak with onset from 200 °C and peaked at 500 °C, similar to Cu oxide reduction, was observed. Quantitative analysis of the TPR profiles suggests that the addition of Cu promoted the reduction of ZnO plate (see the Supporting Information), because there are strong material interactions between Cu and ZnO platelike forms. Methanol synthesis over typical Cu–ZnO catalyst takes place at around 250 °C and thus such facilitated [O] reduction at the materials' interface may be somewhat linked with catalytic performance.

Testing the physical mixture of Cu nanoparticles with rod and plate ZnO, respectively, for hydrogenation of CO_2 was therefore conducted. Table 1 clearly shows a consistently higher selectivity to methanol reaching over 70 % [Eq. (1)] with lesser degree of CO formation from RWGS [Eq. (2)]

Table 1: Catalytic performance of ZnO plate and rod particles mixed with copper and alumina in the synthesis of methanol from hydrogenation of CO_2.[a]

CO_2:H_2 (mole ratio)	T [K]	Catalyst	CO_2 conversion [%]	Methanol selectivity [%]
1:2.2	543	Cu/rod ZnO/Al_2O_3	12.3	42.3
		Cu/plate ZnO/Al_2O_3	10.9	72.7
	553	Cu/rod ZnO/Al_2O_3	15.3	39.1
		Cu/plate ZnO/Al_2O_3	12.0	71.6
1:2.5	543	Cu/rod ZnO/Al_2O_3	15.8	41.0
		Cu/plate ZnO/Al_2O_3	15.5	64.5
	553	Cu/rod ZnO/Al_2O_3	17.8	32.0
		Cu/plate ZnO/Al_2O_3	14.7	63.3

[a] Total flow rate: 40 stp mL min^{-1} at 4.5 MPa.

when ZnO plate is in contact with Cu. In contrast, when the ZnO rod is used, slightly higher CO_2 conversion but much lower methanol selectivity (ca. 40 %), is obtained. Thus, the testing results clearly suggest that the materials' interface between ZnO plate and Cu is crucially essential in methanol production from CO_2 hydrogenation. It is important to elucidate the nature of interactions between ZnO plate and Cu. ZnO is a well known n-type semiconductor (band gap, $E_g \approx 3.3$ eV at 300 K); its mobile electrons at conductive band (CB) may transfer to the Fermi level of metal (i.e. Cu) with high work function at the interface.[12,13]

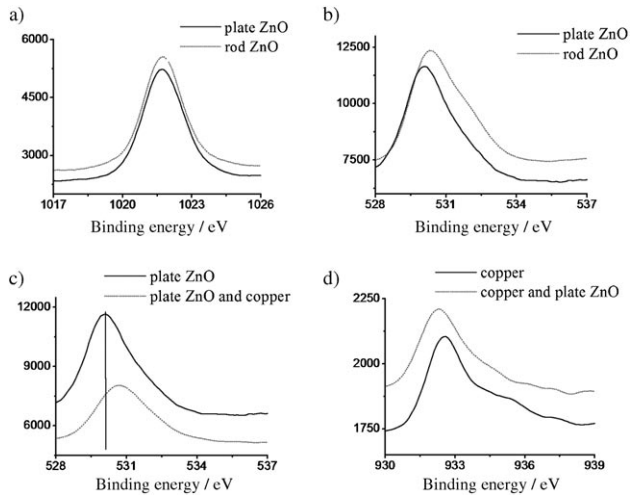

Figure 3. XPS data of a) Zn $2p_{3/2}$; b) O 1s of plate and rod ZnO nanoparticles; c) O 1s of plate ZnO and its mixture with copper; and d) Cu $2p_{3/2}$ of metallic copper and its mixture with plate ZnO.

Characterization of ZnO plate, rod, and their mixture with copper was therefore conducted by X-ray photoelectron spectroscopy (XPS). Figure 3a reveals that the binding energy (BE) of Zn $2p_{3/2}$ is about 1021 eV for all the samples, which agrees with reported Zn^{2+}.[14] However, Figure 3b shows that the BE value of O 1s for the plate sample (530.1 eV) is slightly lower than that of the rod (530.4 eV), implying electrons are easier to be excited from the plate sample. The BE value of O_{1s} of the plate form after addition of Cu reverted to that of rod form (Figure 3c). There is also a corresponding down-shift of Cu $2p_{3/2}$ with reference to 932.8 eV Cu^0 (Figure 3d). In contrast, the BE value of O 1s of the rod sample remains constant regardless of whether it is in contact with Cu (see Figure S2 in the Supporting Information). The [O] terminated polar facet is known to be electron richer than those of nonpolar facets (i.e. 100) that contain equal number of cations and anions.[13] There is indeed electron transfer from ZnO plate to Cu as a result of the formation of a Schottky–Mott junction[12] at the interface, thus affecting the BE values.

Further characterization of ZnO samples with and without Cu using electron paramagnetic resonance (EPR) was carried out. Figure S3 (see the Supporting Information) reveals two intense signals for plate ZnO at $g = 2.00$ and $g = 1.96$, whereas only the former signal at lower intensity is detected for rod sample. The signal at $g = 2.00$ has commonly been assigned to the unpaired electrons deeply trapped in oxygen vacancies, probably via adsorbed oxygen species from air (O_2^-), and the signal at $g = 1.96$ represents unpaired electrons trapped from the CB by shallow donors or impurities.[15] Thus, some strongly and weakly trapped electrons (excited electrons in the CB) were detected on the ZnO polar facets. The plate form appears to give more oxygen defects than the rod form under identical treatment. After the addition of copper, the electron spin count of the signal normalized per milligram of ZnO at $g = 2.00$ showed a marginal change for both types of the ZnO samples, and the signal at $g = 1.96$ decreased substantially in the case of ZnO plate (see Table 2). It is therefore evident that there is electron transfer from the CB of ZnO plate to Cu. Thus, this work offers direct evidence for the existence of strong electronic interactions between the two materials, and the information is complimentary to the XPS data.

Table 2: Quantitative changes of EPR peaks ($g = 2.00$; $g = 1.96$) in the two forms of ZnO and their mixtures with copper normalized per mg of ZnO.

Sample	Spin count [mg^{-1} ZnO], $g = 2.00$	Spin count [mg^{-1} ZnO], $g = 1.96$
Rod ZnO	2.05×10^{13}	0
Cu/rod ZnO	2.71×10^{13}	0
Plate ZnO	6.98×10^{13}	1.51×10^{14}
Cu/plate ZnO	6.14×10^{13}	2.53×10^{13}

The mechanism of methanol synthesis over Cu/ZnO by the syngas route is still controversial despite its industrial practice for many years. The change in the feedstock to CO_2/H_2 will add further complications. It has been proposed that ZnO hosts highly dispersed Cu nanoparticles, which provide exclusively the active sites for methanol production from syngas. However, the nonlinearity frequently observed in correlations of Cu surface area and catalytic activity suggests the existence of a strong Cu–ZnO interaction at various material interfaces.[16] Consequently, Frost stressed the importance of Schottky barrier establishment at the Cu–ZnO interface.[12] According to his view, thermal electrons will flow from the CB of ZnO to the Fermi level of Cu, which facilities the formation of oxygen vacancies by shifting the equilibrium $[O] \rightleftharpoons [\,] + 1/2\,O_2 + 2e^-$, which can account for high activity in methanol synthesis from syngas.[12] Our direct observation of electron transfer from ZnO to Cu at ambient temperature by XPS and EPR analysis is consistent with his mechanism. At elevated temperatures, one would expect more thermal electrons from ZnO to overcome Schottky barrier (estimated to be as low as 0.45 eV[12]) to the copper surface and generate more oxygen vacancies at the materials' interface. This work also contributes two further important points. First, the oxygen atom driven out from the ZnO lattice at the materials' interface is retained in the same mixture (higher reduction peaks in TPR) and seems to have migrated alongside with the electron flow to the copper as surface CuO (redox reaction between the two materials). The TPR results clearly show facilitated oxygen reduction at the interface, possibly the reduction of ZnO via surface Cu oxide by spilled hydrogen (activated on zinc oxide) at much lower temperature. This situation would therefore overcome the above equilibrium constraints in the extent of electron transfer, and the formation of vacancies between the two materials by catalytic reduction. In addition, CO_2 is likely to be activated by the generated vacancies and the Cu phase at the interface assists molecular rearrangement (formate, dioxomethylene, formaldehyde, and methoxy) and hydrogenation to give methanol.[17] Secondly, we have shown that the physiochemical changes at the interface take place primarily between ZnO plate with polar (002) facets and the Cu particle. It is not yet known what unique roles the polar facets play, but these may have arisen from different surface electronic structures.

Clearly, the ZnO plate gives a higher degree of electron trapping as shown in our experiments, which must be intimately related to its defect formation, surface morphology, and electronic properties.[13] Regarding design of future catalysts for the CO_2 hydrogenation reaction, it appears to be crucial to maximize their interfacial area. Without the appropriate interface (for example, nonpolar facets or polar facets in remote distance from Cu), we show that CO_2 can still be activated and hydrogenated on oxygen vacancies of ZnO, but the main products would be CO and H_2O [Eq. (2)], which can be prevalent at high CO_2 coverage under the reaction conditions. Traditionally, it is difficult to gain an understanding of the interface of materials in industrial catalysts.[18] With the introduction of nanosciences to material synthesis, it is shown to be possible to separate complex factors in catalyst formulation (size, shape, support effects) and study them individually in a systematic manner. Herein, we have clearly demonstrated the importance of morphology-controlled SMSI (strong metal–support interaction), which plays a great influence in selectivity for this important reaction.

Experimental Section

The synthesis of platelike ZnO particles was based on the method by Zhu and co-workers.[10] Zinc acetate dihydrate ($Zn(CO_2CH_3)_2{\cdot}2H_2O$, 9.0 g) was dissolved in deionized water (72 mL) and then hexamethylenetetramine ($C_6H_{12}N_4$, 5.76 g) was added. The solution was stirred for 10 min, transferred into a 200 mL teflon-lined autoclave and maintained at 97 °C for 24 h, and then cooled to room temperature slowly. The white precipitate was collected by centrifugation at 5000 rpm for 10 min, after which the supernatant was decanted and discarded. The solid was washed repeatedly with ethanol and water to remove excess precursor. Rodlike ZnO was synthesized according to the method of Liu and Zeng.[11] Zinc nitrate ($Zn(NO_3)_2{\cdot}6H_2O$, 1.487 g) and NaOH (6 g) were dissolved in deionized water (10 mL; molar ratio of Zn^{2+} to OH^- 1:30). Pure C_2H_5OH (100 mL) was added, followed by ethylenediamine ($C_2H_4(NH_2)_2$, 5 mL). The mixed solution was then transferred to a covered plastic container with a volume capacity of 250 mL. The container was kept at room temperature under constant stirring. The length of the rods was controlled by the reaction time: 1 day for the short rods and 3 days for the long ones. After the synthesis, a white crystalline product was centrifuged and washed with deionized water and pure ethanol. The precipitate was dried at 60 °C for 12 h. All the samples were calcined at 723 K for 2 h. The catalysts were prepared by mixing equal quantities of ZnO, Cu, and Al_2O_3 mechanically using pestle and mortar. Cu was synthesized as follows: 0.8 g copper acetate dihydrate ($Cu(CO_2CH_3)_2{\cdot}2H_2O$) was dissolved in ethanol (60 mL) and $NaBH_4$ solution (0.4 g $NaBH_4$ in 10 mL ethanol) was added to reduce Cu^{2+}. The black precipitate was collected by centrifugation at 5000 rpm for 10 min. The solid was washed repeatedly with ethanol and water. The precipitate was dried in vacuum at 100 °C for 2 h. Catalyst tests in the hydrogenation of CO_2 were carried out at a total pressure of 4.5 MPa using a tubular fixed bed reactor (12.7 mm outside diameter) with a catalyst weight of 0.3 g. CO_2/H_2 reaction mixtures with molar ratios of 1:2.2 and 1:2.5 were fed at a rate of 40 stp mL min^{-1} (stp = standard temperature and pressure; $P = 101.3$ kPa, $T = 298$ K) through the catalyst bed. Before each test, the catalyst was pre-reduced in situ at 573 K for 2 h under the H_2 flow (20 stp mL min^{-1}). The products were analyzed by a gas chromatograph equipped with a thermal conductivity detector.

Received: November 12, 2010
Published online: January 20, 2011

Keywords: copper · heterogeneous catalysis · hydrogenation · interfaces · zinc

[1] K. Man, K. Yu, I. Curcic, J. Gabriel, S. C. E. Tsang, *ChemSusChem* **2008**, *1*, 893 – 899.
[2] J. Turner, G. Sverdrup, M. K. Mann, P. C. Maness, B. Kroposki, M. Ghirardi, R. J. Evans, D. Blake, *Int. J. Energy Res.* **2008**, *32*, 379 – 407.
[3] L. K. Rihko-Struckmann, A. Peschel, R. Hanke-Rauschenbach, K. Sundmacher, *Ind. Eng. Chem. Res.* **2010**, *49*, 11073 – 11078.
[4] G. A. Olah, *Angew. Chem.* **2005**, *117*, 2692 – 2696; *Angew. Chem. Int. Ed.* **2005**, *44*, 2636 – 2639.
[5] J. G. Wu, M. Saito, M. Takeuchi, T. Watanabe, *Appl. Catal. A* **2001**, *218*, 235 – 240.
[6] G. C. Chinchen, P. J. Denny, J. R. Jennings, M. S. Spencer, K. C. Waugh, *Appl. Catal.* **1988**, *36*, 1 – 65.
[7] M. Saito, *Catal. Surv. Jpn.* **1998**, *2*, 175 – 184.
[8] R. Narayanan, M. A. El-Sayed, *J. Phys. Chem. B* **2005**, *109*, 12663 – 12676.
[9] A. Mclaren, T. Valdes-Solis, G. Q. Li, S. C. Tsang, *J. Am. Chem. Soc.* **2009**, *131*, 12540 – 12541.
[10] G. R. Li, T. Hu, G. L. Pan, T. Y. Yan, X. P. Gao, H. Y. Zhu, *J. Phys. Chem. C* **2008**, *112*, 11859 – 11864.
[11] B. Liu, H. C. Zeng, *Langmuir* **2004**, *20*, 4196 – 4204.
[12] J. Frost, *Nature* **1988**, *334*, 577 – 580.
[13] H. Morkoç, Ü. Özgür, *Zinc Oxide: Fundamentals, Materials and Device Technology*, 1st ed, Wiley-VCH, Berlin, **2009**.
[14] Y. G. Chang, J. Xu, Y. Y. Zhang, S. Y. Ma, L. H. Xin, L. N. Zhu, C. T. Xu, *J. Phys. Chem. C* **2009**, *113*, 18761 – 18767.
[15] V. Ischenko, S. Polarz, D. Grote, V. Stavarache, K. Fink, M. Driess, *Adv. Funct. Mater.* **2005**, *15*, 1945 – 1954.
[16] K. C. Waugh, *Catal. Lett.* **1999**, *58*, 163 – 165.
[17] S. A. French, A. A. Sokol, S. T. Bromley, C. R. A. Catlow, P. Sherwood, *Top. Catal.* **2003**, *24*, 161 – 172.
[18] T. Ressler, B. L. Kniep, I. Kasatkin, R. Schlogl, *Angew. Chem.* **2005**, *117*, 4782 – 4785; *Angew. Chem. Int. Ed.* **2005**, *44*, 4704 – 4707; and also Y. Lin, Y. Hsu, S. Chen, Y. Lin, L. Chen, K. Chen, *Angew. Chem.* **2009**, *121*, 7722 – 7726; *Angew. Chem. Int. Ed.* **2009**, *48*, 7586 – 7590.

